www.czasopisma.pan.pl PAN POLSKA AKADEMIA NAUK www.journals.pan.pl

Arch. Metall. Mater. **62** (2017), 3, 1511-1520

DOI: 10.1515/amm-2017-0234

P. HYJEK*#, I. SULIMA*, L. JAWORSKA**

# CHARACTERISTICS OF THE NiAl/$Ni_3Al$ MATRIX COMPOSITE WITH $TiB_2$ PARTICLES FABRICATED BY HIGH PRESSURE – HIGH TEMPERATURE SINTERING

The article presents the results of tests carried out on the manufactured composite materials based on a two-phase NiAl/$Ni_3Al$ matrix, which was enriched with the addition of $TiB_2$ ceramic particles added in an amount of 4 and 7 vol%. The resulting mixtures were sintered by the High Pressure High Temperature (HP-HT) process. The results were compared to the results obtained for the sole matrix material produced under the same conditions. It has been shown that, at a lower density, the addition of reinforcing particles increases the composite hardness, Young's modulus and resistance to frictional wear. However, higher addition of $TiB_2$ (7 vol%) was observed to yield less satisfactory results, and despite higher hardness and lower density caused a decrease in other properties tested. The produced materials were characterized by a compact and highly differentiated microstructure free from any noticeable cracks and pores.

*Keywords:* Sintering, High Pressure High Temperature process, Metal matrix composites, tribological properties

## 1. Introduction

Modern technology poses new challenges to materials engineering. This mainly refers to the design and technology for the manufacture of materials with different chemical and phase composition. These materials are expected to offer higher and more stable mechanical properties than the materials used currently. The materials selected for tests belong to a group of alloys based on the intermetallic Ni-Al phase. The system includes five different phases, but in terms of the properties possessed only NiAl and $Ni_3Al$ can find industrial applications. The most important are the following properties: a relatively high melting point and Young's modulus, high resistance to oxidation and low density (favourable specific strength $R_m/\rho$), relatively low friction wear and sufficiently high resistance to the effect of chemicals [1-3]. A combination of these features decides that the above mentioned phases are used as a base material for multicomponent alloys, mainly those designed for operation at high temperatures [4]. In numerous alloys, the $Ni_3Al$ phase is also used as a reinforcing element [5,6]. The major drawbacks of the NiAl phase include its brittleness at room temperature and unsatisfactory creep resistance at elevated temperatures [7-9]. The drawbacks of the $Ni_3Al$ phase are higher density (7.5 g/$cm^3$) and lower resistance to oxidation compared to NiAl, and also low fracture toughness [3,10,11]. Much effort has been made to improve these imperfections, and the main tool used was modification of microstructure. To achieve this goal, various alloying additions were introduced to induce precipitation of the second phase, or solid particles of the ceramic material were added [12]. The grains were refined or their morphology was changed (lamellar vs dendritic). Different manufacturing methods were applied, including casting and sintering, and in many cases, positive results were obtained. As a next step, the ready sinters were examined, and it has turned out that the fine-grain Ni-Al alloy gives satisfactory results in terms of the improved ductility at room temperature, offering, moreover, higher hardness, strength and fracture toughness [13-16]. High values of the Young's modulus and strength were also achieved owing to the addition of $TiB_2$ introduced in an amount of up to 30% [17,18]. Since the time when it was demonstrated that the two-phase NiAl/$Ni_3Al$ system has the properties superior to the properties of each of these two phases considered separately [19,20], the resultant alloy has become the object of numerous studies. Another method for hardening a two-phase NiAl/$Ni_3Al$ matrix consists in the introduction of fine ceramic particles uniformly distributed therein. Beneficial effects of this operation have already been shown for alloys [21] and mono-phase NiAl [18,22,23] as well as $Ni_3Al$ [24,25] systems.

When NiAl and $Ni_3Al$ alloys were selected for the composite matrix, a satisfactory oxidation resistance of the former one and excellent strength at elevated temperatures of the latter one were taken into consideration. In contrast, $TiB_2$ can offer

* PEDAGOGICAL UNIVERSITY, INSTITUTE OF TECHNOLOGY, CRACOW, POLAND
** AGH UNIVERSITY OF SCIENCE AND TECHNOLOGY, FACULTY OF NON-FERROUS METALS, AL.A. MICKIEWICZA 20, 30-059 KRAKOW, POLAND
# Corresponding author: phyjek@up.krakow.pl

high melting point, hardness and Young's modulus, low density, satisfactory resistance to oxidation, chemical and structural stability at high temperatures and compatibility with nickel aluminides [26,27]. It is therefore expected that the composite material based on a two-phase NiAl/$Ni_3Al$ matrix reinforced with $TiB_2$ will be suitable for various applications, including high-temperature use and conditions demanding improved resistance to abrasion.

## 2. Materials and methods

The test material was prepared by high pressure – high temperature sintering (HP-HT) in a Bridgman-type apparatus. The starting material was NiAl/$Ni_3Al$ powder (Ni79Al21, Goodfellow) of 45-150 μm granulation. According to the manufacturer's specification, the melting point of this powder is 1530°C. The $TiB_2$ powder (Atlantic Equipment Engineers) of 2-10 μm granulation was added in an amount of 4 vol% and 7 vol%. The whole was mixed with grinding steel balls for 6 hours in a Turbula device to achieve a uniform distribution of the ceramic particles. The main objective in the fabrication of composites of this type is providing a uniform distribution of ceramic particles (in this case of $TiB_2$) in the matrix and producing a dense microstructure without microcracks and pores, characterized by strong cohesive bonds formed between the grains. An important factor shaping the properties of the resulting composite is the manufacturing process carried out in a Bridgman type pressure apparatus. The conducted studies have confirmed that free sintering of this material is impossible due to the matrix hardening effect at the stage of mixture preparation, which makes moulding of samples very difficult. The HP-HT process is very effective in the improvement of grain orientation compared to the conventional hot pressing and hot isostatic pressing methods, providing a density reaching 99% of the theoretical density [28,29]. The HP-HT process has already proved to be successful in the manufacture of, among others, 316L steel [29,30], NiAl alloy [31] and NiAl+$TiB_2$ composite [32].

A scheme of the sintering process using Bridgman type apparatus was presented in [31,32]. The pre-moulded mixtures were placed in a graphite heater and then in a special reactive material, providing electrical contact and pseudoisostatic sintering conditions. Samples were sintered at a pressure of 7.5 ±0.2 GPa. The sintering temperature was 1504°C. The duration of the process was 60 seconds. The samples produced had a diameter of 15 mm and a thickness of 5 mm.

The starting composition of the composite mixtures as well as the sintering process parameters are given in Table 1. Figure 1 shows a morphology of the initial matrix and reinforcing phase powders used in the composite manufacturing. The grain size is consistent with the values stated by the manufacturer, i.e. 45-150 μm (Fig. 1a) for NiAl and 2-10 μm (Fig. 1b,c) for $TiB_2$. The morphology of powders varies, showing much finer grains of a lamellar type in the NiAl powder than the values given by the manufacturer. On the other hand, large grains, especially grains approaching their maximum size, occur sporadically and have a globular shape. The observed shape of $TiB_2$ grains is polyhedral in the case of larger grains and lamellar in the case of smaller grains.

The evaluation of the effect of $TiB_2$ particles added in an amount of 4 and 7 vol% to the NiAl/$Ni_3Al$ matrix was based on the results of the measurements of density, Young's modulus and Vickers hardness. The density was measured by hydrostatic method. The uncertainty of measurement was 0.02 g/$cm^3$. Young's modulus was determined with an Panametrics Epoch III ultrasonic flaw detector. The value of error was 2%. Vickers hardness HV1 was determined with a NEXUS 4000 hardness tester. Phase identification were made by X-ray diffraction (XRD) using Cu Kα radiation with a scintilation detector (Brucker Discover D8). Microstructural examinations were conducted on the obtained composites, using an Olympus GX-51 optical microscope with Nomarski contrast and JEOL JSM 6610 LV scanning electron microscope with **E**nergy **D**ispersive **S**pectroscopy (AZtec). The examinations allowed determining, among others, the homogeneity, compactness and porosity of the composites. Measurements covered the uniformity of $TiB_2$ particles distribution in matrix, particle size, and the shape and homogeneity of composite phases.

Studies also included the assessment of wear resistance of the obtained composite materials. Tests were conducted in an ELBIT universal material tester operating according to the relevant standard parameters [33]. Using a ball-on-disc/Pin-On-Disc test principle, the device is designed for studies of the high velocity wear behaviour in a couple of materials operat-

TABLE 1

Parameters of the pressure-assisted sintering process of two-phase NiAl/$Ni_3Al$ alloy and composite based on this alloy

| Samples | Pressure [GPa] | Temperature [°C] | Sintering time, [s] | Poisson's ratio |
|---|---|---|---|---|
| NiAl/$Ni_3Al$ matrix | 7.5 | 1504 | 60 | 0.36 |
| NiAl/$Ni_3Al$ + 4 vol% $TiB_2$ | | | | |
| NiAl/$Ni_3Al$ +7 vol% $TiB_2$ | | | | |

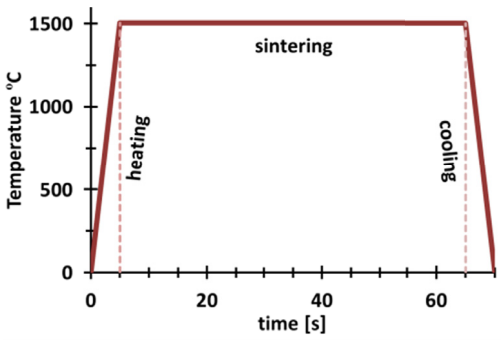

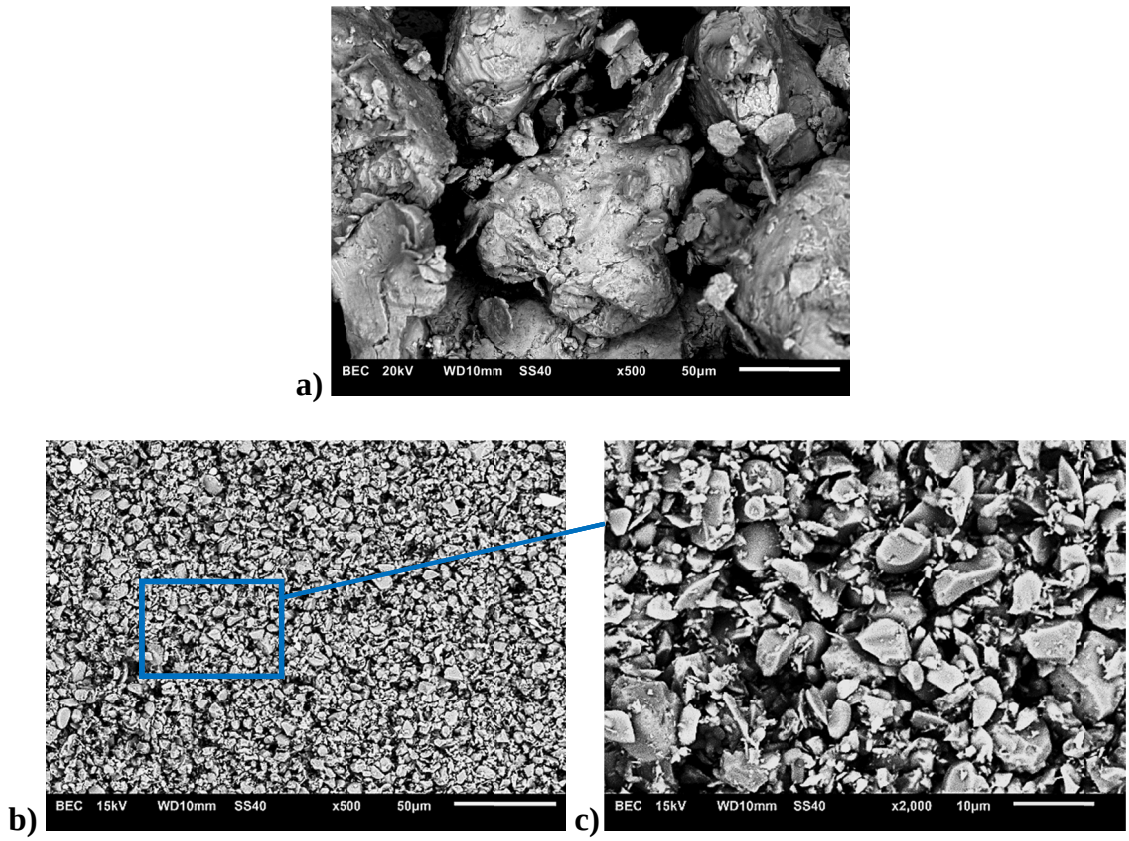


Fig. 1. Powder morphology: a) Ni79Al21 (Goodfellow) and b, c) $TiB_2$ (AEE) at two different magnifications, BSE, SEM

ing at high temperatures. The following test parameters were applied:

- Load applied: F = 5 N
- Radius of the wear track: R – 5 mm
- Environment: Air
- Ball diameter: r – 1/8", $Al_2O_3$
- Temperature: 24 ±2 °C
- Velocity: V = 0.1 m/s
- Test duration: 10000 s

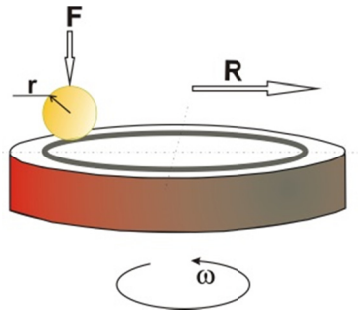


Using $Al_2O_3$ grinding balls and a load of 5 N, parameters such as the coefficient of friction, furrow depth (the depth of material loss) and the wear rate W were determined. The coefficient of friction and furrow depth were measured automatically and recorded in real time by a computer system of the tribotester. The wear rate was determined as a wear volume according to the relevant standard [34]:

$$W = V/(F * L), \quad (1)$$

where: $W$ – specific wear rate; $V$ – is the wear volume on disc specimen, in cubic milimetres, $F$ – is the applied load, in newtons; $L$ – is the sliding distance, in metres.

The loss of volume was determined from the measurements of the wear track width according to a precise relationship ("The exact equation") specified in the relevant standard [29]. The wear track width was measured by optical microscopy. For the tested materials Wear track width/sphere radius <0.3 (correct to 1%).

The calculated values of the specific wear rate were compared with the values calculated using relationships provided by other authors. The impact of factors, such as moisture content, load value and type of grinding balls on the coefficient of friction and wear volume has already been tested and described in [35-37].

## 3. Results and discussion

Figure 2 shows microstructure of the obtained sinters (both matrix and composites) examined under an optical microscope. The produced materials, both NiAl and $NiAlTiB_2$, are characterized by compact although relatively diversified structure, especially intragranular, with a negligible amount of pores. In composite materials with 4 and 7 vol% $TiB_2$, areas of the size of less than 10 µm were observed at grain boundaries; their presence was not detected in the matrix material. The uniformity of distribution of these areas (particles) in the matrix was satisfactory, contrary to the uniformity of distribution of other phases occurring in the NiAl and $NiAlTiB_2$ systems.

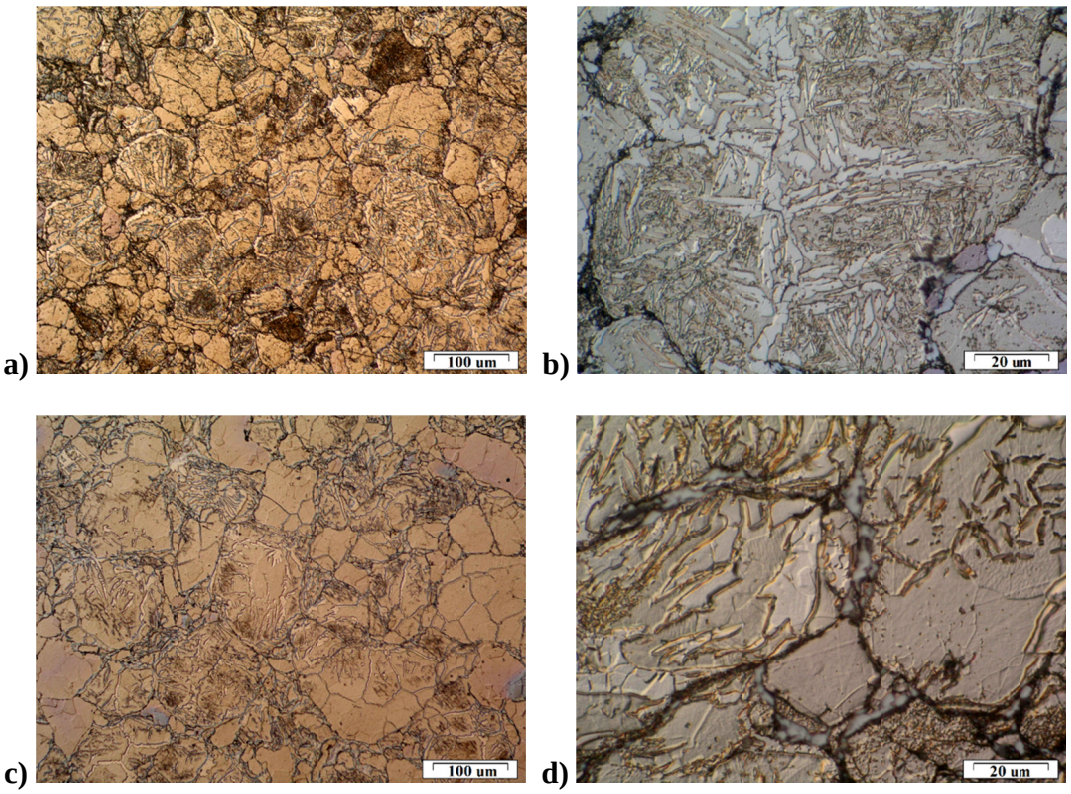


Fig. 2. LM micrograph of NiAl/$Ni_3Al$ matrix composite with $TiB_2$ content of: a, b) 4 vol% at two different magnifications and c, d) 7 vol% at two different magnifications, Nomarski contrast

Similar analogies were derived from the studies carried out by scanning electron microscopy. Figure 3 shows the microstructure and distribution of various phases, including $TiB_2$ particles. The analysis of selected areas of the microstructure is shown in Figure 4. Individual grains are composed of areas where in the dark background (aluminium content of about 40 at% corresponding to the NiAl phase) are embedded in a non-uniform manner (forming sometimes an „acicular" pattern) light-colour

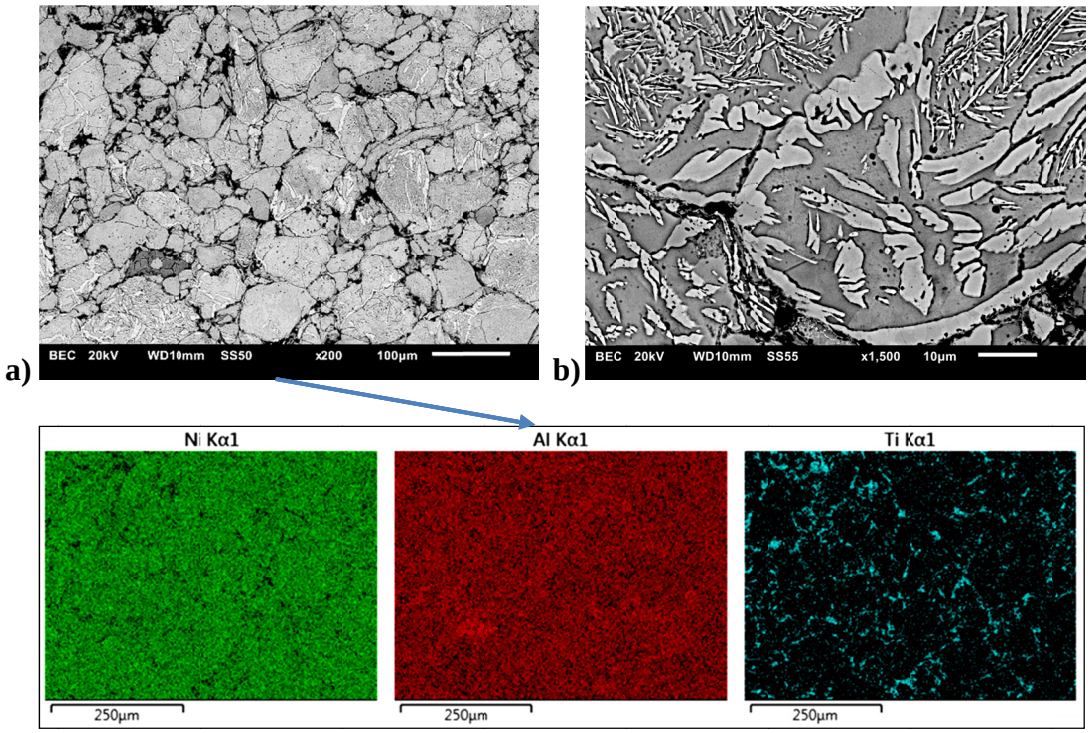


Fig. 3. Microstructure and corresponding distribution maps of elements such as Ni, Al, Ti, in NiAl/$Ni_3Al$ + 4 vol% $TiB_2$ composite at two different magnifications a) and b), BSE, SEM

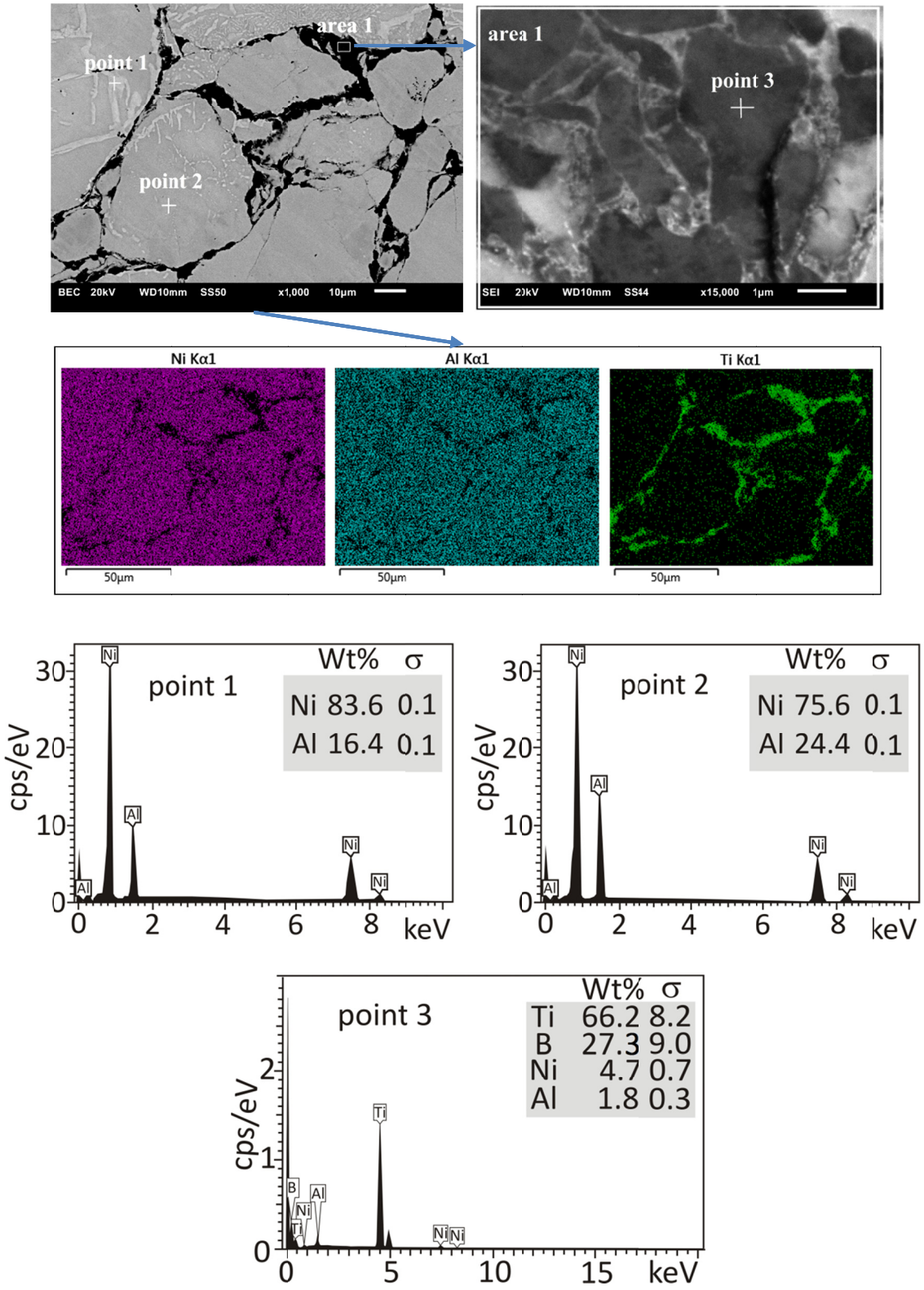


Fig. 4. Analysis of selected areas of the microstructure in NiAl/$Ni_3Al$ + 7 vol% $TiB_2$ composite (BSE), area 1 – microstructure area at a magnification, SEI, SEM

areas containing aluminium in an amount of about 23 at%, which corresponds to the $Ni_3Al$ phase. Additionally, at grain boundaries, areas rich in titanium, or in titanium and boron have been identified. Their size corresponds to the size of the grains of $TiB_2$ powder (2-10 µm) introduced into the matrix. These sinters are characterized by low porosity observed in different composites (Figs. 2-4). No significant differences resulting from the added $TiB_2$ were observed.

Figure 5 shows the results of the XRD phase analysis of composite with 4 vol% $TiB_2$ (a) and 7 vol% $TiB_2$ (b). The analysis has revealed in the fabricated materials the presence of the following phases: NiAl, $Ni_3Al$ and $TiB_2$.

The results of studies of the physical properties (density and Young's modulus) are shown in Figure 6a. The density of the manufactured composites depends largely on the amount of the introduced ceramic particles of $TiB_2$. This is due to the lower density of the ceramic particles (4.52 g/cm$^3$ [38]) as compared to the density of the intermetallic phases of NiAl (5.86 g/cm$^3$ [1]) and $Ni_3Al$ (7.5 g/cm$^3$). Consequently, the density of the manufactured composites was decreasing in proportion to the amount of the introduced particles (4 and 7 vol%), assuming the values of 6.55 g/cm$^3$ and 6.27 g/cm$^3$, respectively, while the density of the two-phase NiAl/$Ni_3Al$ material was 6.61 g/cm$^3$. The values of Young's modulus increased slightly in individual composites with the increasing amount of $TiB_2$ introduced to the matrix, but in spite of this, the final result was considered unsatisfactory. To some extent it was also due to the low Young's modulus of the matrix. Failure to obtain satisfactory results was even more evident, when Young's modulus values obtained in the sintered $Ni_3Al$/NiAl system were compared with analogical values obtained for the NiAl and $Ni_3Al$ phases separately (188 GPa and 168 GPa, respectively) [39-41], and when it was additionally stated that in [17] the increasing content of $TiB_2$ resulted in a considerable increase of this parameter.

The results of hardness (HV1) measurements are shown in Figure 6b. Hardness was observed to increase depending on the addition of $TiB_2$. The average value was 445 HV1 for the matrix, for the composite with 4 vol% $TiB_2$ it was 500 HV1 and 540 HV1 for the composite with 7 vol% $TiB_2$. Despite the large scatter of the measured values observed sometimes and resulting from the highly diversified structure (two-phase matrix and ceramic particles), differences in the results of the hardness HV1 measurements are significant. The effect of structure variations on the properties has already been described in [31 and 32].

The results of abrasive wear resistance tests carried out by the ball-on-disc method are shown in Figure 7. Adding 4 vol% of the $TiB_2$ ceramic particles raised the values of the friction coefficient compared with the values obtained for the sole matrix. A similar relationship was found and proved in [37]. Higher amount of the added $TiB_2$ (7 vol%) was found to reduce the coefficient of friction compared to the 4 vol% addition. This is reflected in the values of the wear rate and in the respective size of furrows. Composites with higher coefficient of friction showed lower wear rate as documented by the smaller depth and width of furrows. Similar values of the specific wear rate were obtained when this parameter was calculated from the relationship proposed by Ozdemir [35]. The difference in the results was insignificant and the wear rate was lower by 4.25-6.3%. The difference is strictly related with the wear rate of a given material. The higher is the wear rate, the larger is the difference in the results. Some attention also deserves the irregular character of the friction coefficient curves plotted in relation to time. The source of these irregularities should be sought in the complex and uneven structure of materials tested.

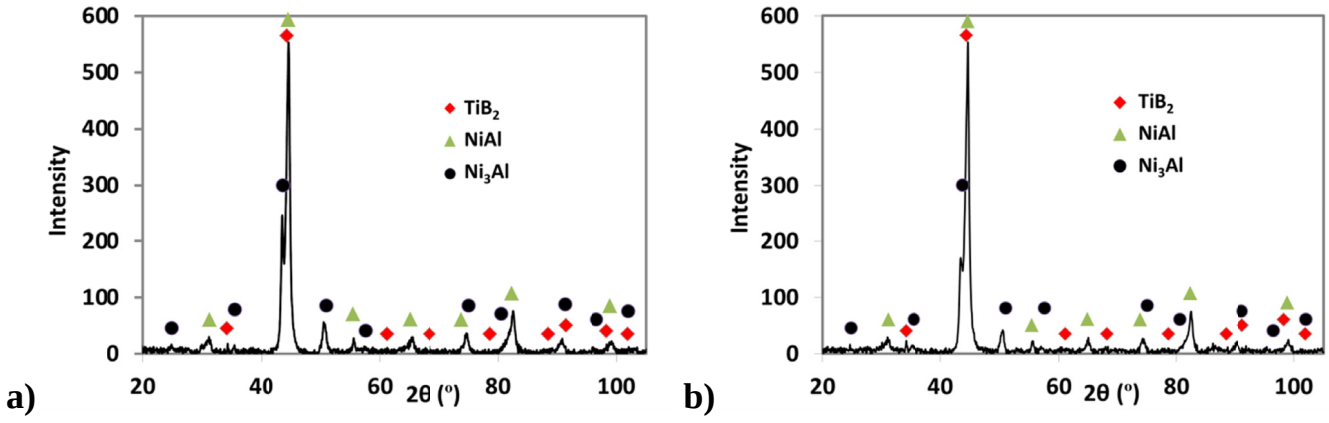


Fig. 5. The results of XRD phase analysis of the composite with $TiB_2$ content of: a) 4 vol%, and b) 7 vol%

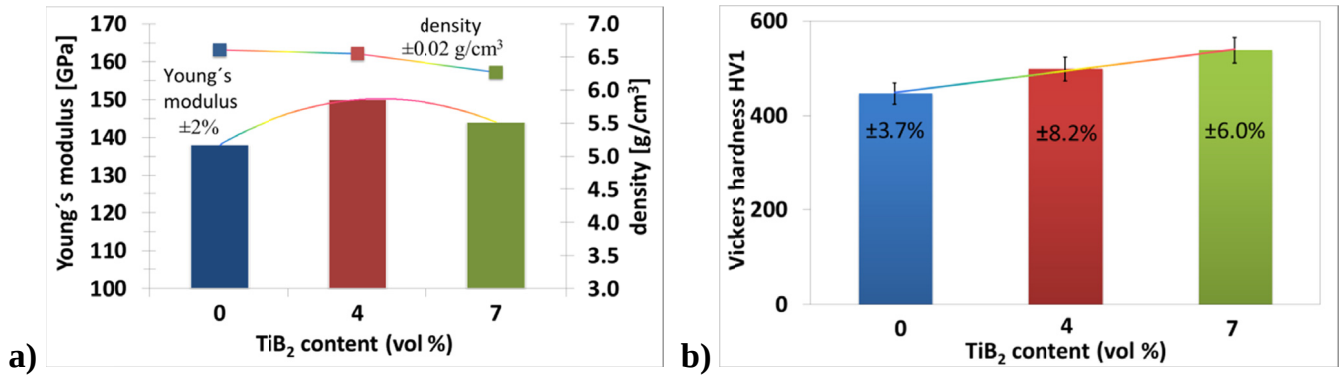


Fig. 6. The results of: a) Young's modulus and density, and b) Vickers hardness of the NiAl/$Ni_3Al$ matrix with various $TiB_2$ content

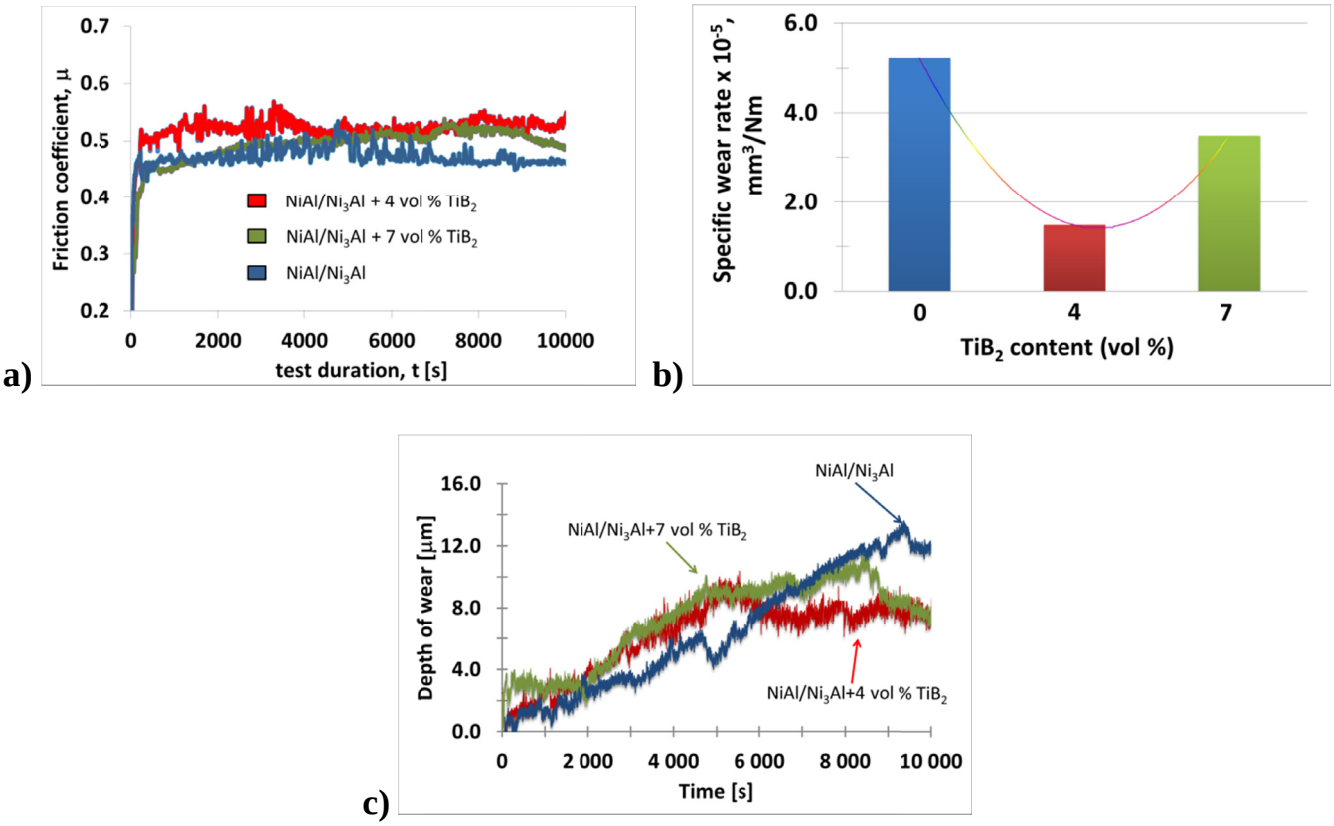


Fig. 7. The results of tibological tests: a) friction coefficient vs time, b) specific wear rate dependence on $TiB_2$ content, c) furrow depth vs time

Interesting information can be drawn from the furrow depth vs time chart (Fig. 7c). The matrix shows a relatively even wear over the whole test duration (10000 s). In composites, a similar mechanism of wear, i.e. the formation of furrows, was observed. After a certain lapse of time (about 5000 seconds for both composites), the wear rate was stabilized, which means that the material showed no wear any longer. Probably it was caused by the material strengthening effect, which might be due to the seizure of particles detached previously (Figs. 9,10), although composite with 7 vol% content of the reinforcing particles showed some symptoms of stability as early as during 500-2000 seconds.

From the above it can be concluded that in the tested materials, it is the coefficient of friction that mainly controls the wear rate. The $NiAl/Ni_3Al$ alloy shows the highest rate of wear (the lowest coefficient of friction in the range of 0.45-0.50), while the same alloy with 4 vol% $TiB_2$ shows the lowest rate of wear (the highest coefficient of friction in the range of 0.50-0.55). It seems that the addition of 7 vol% $TiB_2$ introduces too many reinforcing particles to the composite matrix. The high content of this addition pushes the reinforcing particles to the area of grain boundaries, where the excessive amount of these particles often results in their non-uniform distribution. Although in this particular case, large concentrations of the reinforcing particles

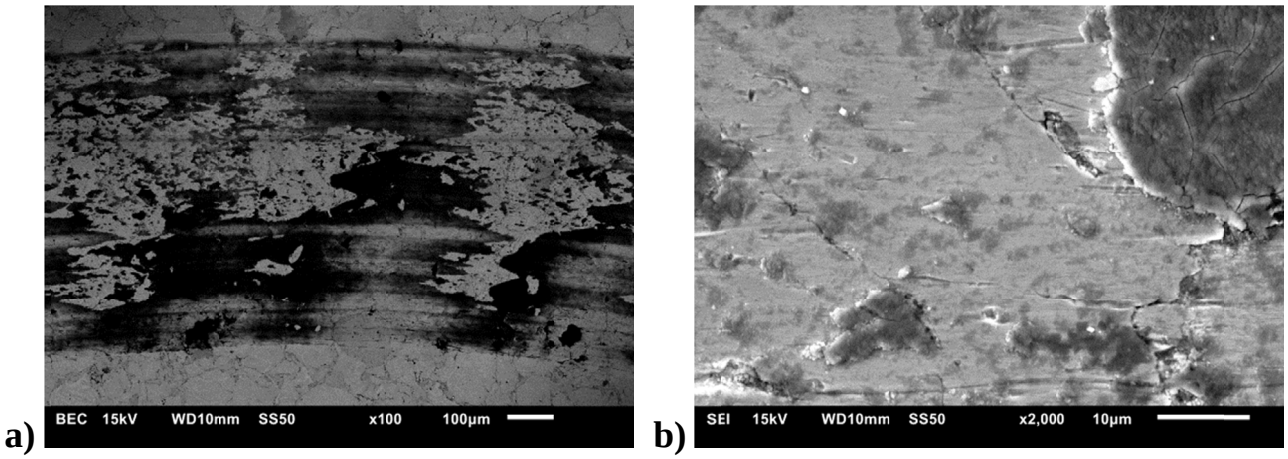


Fig. 8. Surface microstructure after ball-on-disc friction test of $NiAl/Ni_3Al$ matrix at two different magnifications a) BSE and b) SEI, SEM

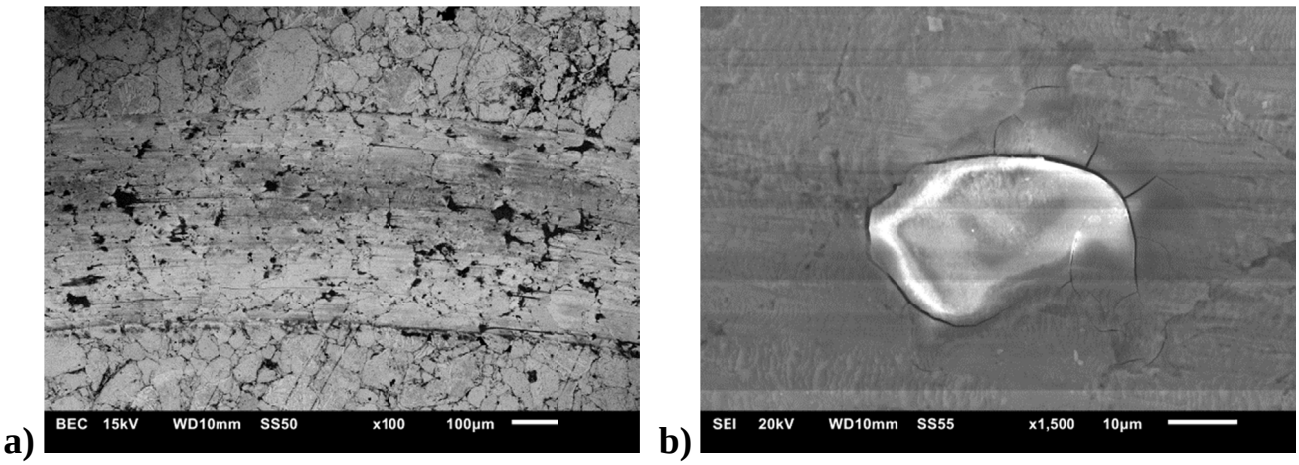


Fig. 9. Surface microstructure after ball-on-disc friction test of NiAl/$Ni_3Al$ + 4 vol% $TiB_2$ composite at two different magnifications a) BSE and b) SEI, SEM

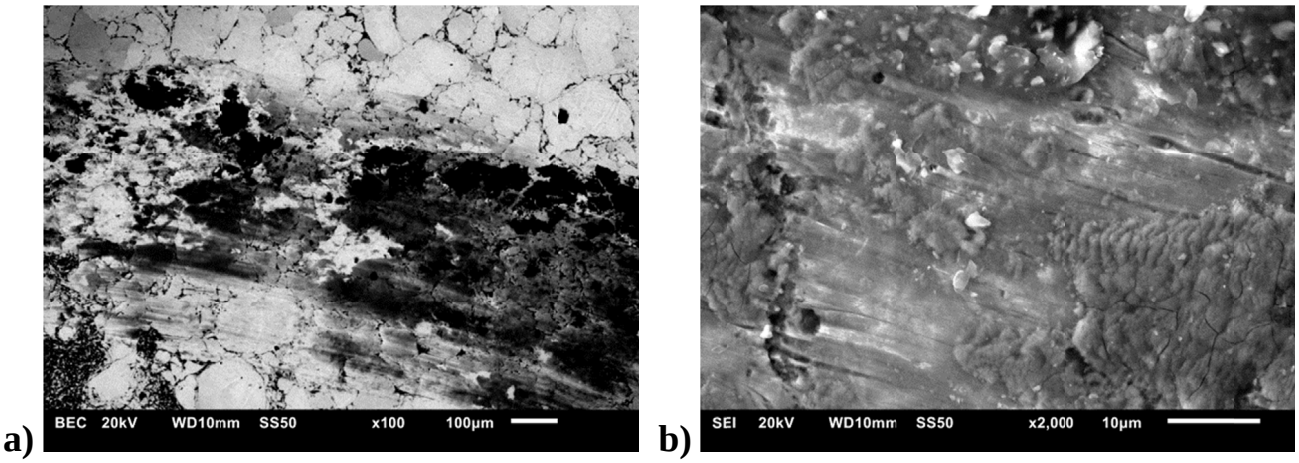


Fig. 10. Surface microstructure after ball-on-disc friction test of NiAl/$Ni_3Al$ + 7 vol% $TiB_2$ composite at two different magnifications a) BSE and b) SEI, SEM

were not observed, and their relatively even distribution at grain boundaries was reported, it can not be ruled out that the situation might be different in, for example, the sample cross-section. In any case, the uniformity of distribution was definitely much better in the composite with 4 vol% $TiB_2$. In the composite with 7 vol% $TiB_2$, the reinforcing particles were observed to contact each other (Figs. 2d and 4) – the effect which did not occur in the case of the 4 vol% addition of $TiB_2$, and most probably this effect was responsible for higher wear in the composite with 7 vol% addition of $TiB_2$. The reason should be sought in too large differences between the size of the Ni79Al21 grains (45-150 µm) and $TiB_2$ particulate (2-10 µm). The result is the limited number of "unoccupied" sites at the matrix boundary, where the reinforcement particles could be embedded. Therefore, further studies in this field will focus on the use of smaller particles of the NiAl powder added to the composite, or on searches for the optimal size of the reinforcing particles introduced to the matrix.

Examinations of the surfaces exposed to the effect of abrasion have indicated an abrasive-friction nature of wear. Figures 8-10 show these surfaces with the characteristic points of wear. Well visible is plastic deformation and cracks. The EDS analysis has confirmed the effect of oxidation taking place on the surfaces exposed to friction. The oxides formed are probably those of NiO and $Al_2O_3$. This indicates that one of the wear mechanisms is the abrasive wear that arises in the area of friction due to the oxidation of wear products. Cracks observed in the tracks of wear are probably the result of the presence of hard oxides and their inherent brittleness (Fig. 9b). The results of the evaluation of the volume of material removed in the ball-on-disc test correspond to the results of measurements of the width of the wear tracks made during the examinations conducted by optical and scanning electron microscopy.

## 4.Conclusions

The applied production parameters T = 1504°C and P = 7.5 GPa allowed obtaining compact though structurally diverse material. This has a significant impact on the scatter of properties not only within the material itself but also within its individual grains. The observed effect is the result of a two-phase structure of the NiAl/$Ni_3Al$ matrix. In spite of this, the High

Pressure-High Temperature method appears to be a tool quite effective in the manufacture of intermetallic phases included in the Ni-Al system and composites with the matrix based on these phases. The introduction of 4 and 7 vol% $TiB_2$ addition to the two-phase matrix was observed to raise the composite strength and tribological properties. The composite with 7 vol% $TiB_2$ was characterized by higher hardness but also higher wear rate compared to the composite with 4 vol% $TiB_2$. It was also characterized by a lower value of the Young's modulus. The density of the composites was decreasing in proportion to the addition of $TiB_2$.

**Acknowledgements**

This work was carried out with financial support through statutory funds of Pedagogical University in Cracow.

Apparatus co-financed by the European Regional Development Fund under the Infrastructure and Environment Programme: "For the Development of the Infrastructure and environment"

## REFERENCES

[1] C.T. Liu, Recent advances in ordered intermetallics, Materials Chemistry and Physics **42**, 77-86 (1995).

[2] S.C. Deevi, V.K. Sikka, C.T. Liu, Processing, properties, and applications of nickel and iron aluminides, Progress in Materials Science **42**, 177-192 (1997).

[3] C.M. Ward-Close, R. Minor & P.J. Doorbar, Intermetallic-matrix composites-a review Intermetallics **4**, 217-229 (1996).

[4] K. Bochenek, M. Basista, Advances in processing of NiAl intermetallic alloys and composites for high temperature aerospace applications, Progress in Aerospace Sciences **79**, 136-146 (2015).

[5] J.W. Choi, Y.M Kong, H.E. Kim, I.S. Lee, Reinforcement of Hydroxyapatite Bioceramic by Addition of $Ni_3Al$ and $Al_2O_3$, Journal of the American Ceramic Society **81**, 1743-1748 (1998).

[6] B. Torres, M. Lieblich, J. Ibáñez, A. García-Escorial, Mechanical properties of some PM aluminide and silicide reinforced 2124 aluminium matrix composites, Scripta Materialia **47**, 45-49 (2002).

[7] M.T. Perez-Prado, M.E. Kassner, Chapter 9-Creep of Intermetallics, Fundamentals of Creep in Metals and Alloys (Third Edition), 189-232 (2015).

[8] R. Darolia, NiAl Alloys for High. Temperature Structural Applications, JOM **43**, 44-49 (1991).

[9] D.B. Miracle, Overview No. 104 The physical and mechanical properties of NiAl, Acta Metallurgica et Materialia **41**, 649-684 (1993).

[10] V.K. Sikka, S.C. Deevi, S. Viswanathan, R.W. Swindeman, M.L. Santella, Advances in processing of Ni3Al-based intermetallics and applications, Intermetallics **8**, 1329-1337 (2000).

[11] E.P. George, C.T. Liu, D.P. Pope, Intrinsic ductility and environmental embrittlement of binary $Ni_3Al$, Scripta Metallurgica et Materialia **28**, 857-862 (1993).

[12] C. Suryanarayana, Nasser Al-Aqeeli, Mechanically alloyed nanocomposites, Progress in Materials Science **58**, 383-502 (2013).

[13] G. Sauthoff, Multiphase intermetallic alloys for structural applications, Intermetallics **8**, 1101-1109 (2000).

[14] D.E. Alman, N.S. Stoloff, Powder fabrication of monolithic and composite NiAl, International Journal of Powder Metallurgy **27**, 29-41 (1991).

[15] C.C. Koch, Intermetallic matrix composites prepared by mechanical alloying - a review, Materials Science and Engineering: A **244**, 39-48 (1998).

[16] S. Wang, D. He, Y. Zou, J. Wei, L. Lei, Y. Li, J. Wang, W. Wang, and Z. Kou, High-pressure and high-temperature sintering of nanostructured bulk NiAl materials, Journal of materials research **24**, 2089-2096 (2009).

[17] R.K. Viswanadham, S.K. Mannan, K.S. Kumar, A. Wolfenden, Elastic modulus of NiAl-TiB2 composites in the temperature range 300 to 1273 K, Journal of Materials Science Letters **8**, 409-410 (1989).

[18] J.D. Whittenberger, R.K. Viswanadham, S.K. Mannan, B. Sprissler, Elevated temperature slow plastic deformation of NiAl-TiB2 particulate composites at 1200 and 1300K, Journal of Materials Science January **25**, 35-44 (1990).

[19] R.S. Polvani, W.S Tzeng and P.R. Strutt, High temperature creep in a semi-coherent NiAl-Ni2AlTi alloy, Metallurgical and Materials Transactions A **7**, 33-40 (1976).

[20] S. Guha, P.R. Munroe, I. Baker, Room temperature deformation behavior of multiphase Ni- 20at.% Al- 30at.% Fe and its constituent phases, Materials Science and Engineering: A **131**, 27-37 (1991).

[21] I. Sulima., P. Putyra, P. Hyjek, T. Tokarski, Effect of SPS parameters on densification and properties of steel matrix composites, Advanced Powder Technology **26**, 1152-1161 (2015).

[22] A.A. Shokati, N. Parvin, M. Shokati, Combustion synthesis of NiAl matrix composite powder reinforced by TiB2 and TiN particulates from Ni–Al–Ti–BN reaction system, Journal of Alloys and Compounds **585**, 637-643 (2014).

[23] D. Kalinski, M. Chmielewski, K. Pietrzak, K. Choregiewicz, An influence of mechanical mixing and hot-pressing on properties of NiAl/Al2O3 composite, Archives of Metallurgy and Materials **57**, 695-702 (2012).

[24] E. Fraś, A. Janas, P. Kurtyka, S. Wierzbiński, Structure and properties of cast Ni3Al/TiC and Ni3Al/TiB2 composites. Part II. Investigation of mechanical and tribological properties and of corrosion resistance of composites based on intermetallic phase Ni3Al reinforced with particles of TiC and TiB2, Archives of Metallurgy and Materials **49**, 113-141 (2004).

[25] N.S. Stoloff, D.E. Alman, Innovative Processing Techniques for Intermetallic Matrix Composites, MRS Bulletin, 47-53 (1990).

[26] J.R. Ramberg, W.S. Williams, High temperature deformation of titanium diboride, Journal of Materials Science **22**, 1815-1826 (1987).

[27] J.A. Moser, M. Aindow, W.A.T. Clark, S. Draper, H.L. Fraser, Compatibility of potential reinforcing ceramics with Ni and Fe aluminides, Intermetallic matrix composites, MRS Symposium, 379-384 (1990).

[28] P. Klimczyk, L. Jaworska, V. Urbanovich, Mechanical Properties of Si3N4/SiC Composites With Various Additions, Acta Metallurgica Slovaca **17**, 90-98 (2011).

[29] I. Sulima, R. Kowalik, Microstructure, corrosion behaviors and mechanical properties of the steel matrix composites fabricated by HP-HT method, Materials Science and Engineering: A **639**, 671-680 (2015).

[30] I. Sulima, Consolidation of AISI316L Austenitic Steel - TiB2 Composites by SPS and HP-HT Technology, Sintering Techniques of Materials, ed. by Arunachalam Lakshmanan, Rijeka, InTech-Open Access Publisher; Chapter **7**, 125-153 (2015).

[31] P. Hyjek, I. Sulima, P. Malczewski, L. Jaworska, Application of HP-HT method in the manufacture of NiAl phase, Journal of Achievements in Materials and Manufacturing Engineering **55**, 700-705 (2012).

[32] P. Hyjek, I. Sulima, P. Figiel, NiAl composite reinforced with TiB2 ceramic particles, Innovative Manufacturing Technology 2013, ed. by Magdalena Szutkowska, 31-42 (2013).

[33] ASTM G99-05, American Society for Testing and Materials, Standard Test Method for Wear Testing with a Pin-on-Disk Apparatus, (1995).

[34] ISO 18535:2016, Diamond-like carbon films – Determination of friction and wear characteristics of diamond-like carbon films by ball-on-disc method, (2016).

[35] O. Ozdemir, S. Zeytin, C. Bindal, Tribological properties of NiAl produced by pressure-assisted combustion synthesis, Wear **265**, 979-985 (2008).

[36] Ş. Taktak, M.S. Başpınar, Observation of delamination wear of lubricious tribofilm formed on Si3N4 during sliding against WC--Co in humidity air, Tribology International **39**, 39-49 (2006).

[37] Y. Xiao, X. Shi, W. Zhai, J. Yao, Z. Xu, L. Chen, and Q. Zhu, Tribological Performance of NiAl Self-lubricating Matrix Composite with Addition of Graphene at Different Loads, Journal of Materials Engineering and Performance **24**, 2866-2874 (2015).

[38] R. Riedel, Handbook of ceramic hard materials, Weinheim, Wiley--Vch Verlag GmbH **2**, 968-990 (2000).

[39] D.B. Miracle, R. Darolia, NiAl and its Alloys, Structural Applications of Intermetallic Compounds, ed. by J.H. Westbrook and R.L. Fleischer, 55-74 (1995).

[40] N.S. Stoloff, V.K. Sikka (eds.), Physical metallurgy and processing of intermetallic compounds, Chapman & Hall, New York (1996).

[41] G.K. Dey, Physical metallurgy of nickel aluminides, Sadhana **28**, 247-262 (2003).